

## Supporting Information (SI) Appendix

### Shift from androgen to estrogen action causes abdominal muscle fibrosis, atrophy, and inguinal hernia in a transgenic male mouse model

Hong Zhao<sup>a</sup>, Ling Zhou<sup>a</sup>, Lin Li<sup>b</sup>, John Coon V<sup>a</sup>, Robert T. Chatterton<sup>a</sup>, David C. Brooks<sup>a</sup>, Enze Jiang<sup>a</sup>, Li Liu<sup>d</sup>, Xia Xu<sup>e</sup>, Zhiyong Dong<sup>a</sup>, Francesco J. DeMayo<sup>f</sup>, Jonah J. Stulberg<sup>c</sup>, Warren G. Tourtellotte<sup>b</sup>, and Serdar E. Bulun<sup>a, 1</sup>

<sup>a</sup>Department of Obstetrics and Gynecology (Division of Reproductive Science in Medicine), <sup>b</sup>Department of Pathology (Division of Neuropathology), and <sup>c</sup>Department of Surgery (Gastrointestinal/Endocrine Division), Feinberg School of Medicine, Northwestern University, Chicago, Illinois, USA. <sup>d</sup>The First Affiliated Hospital of Nanjing Medical University, Nanjing, Jiangsu, China. <sup>e</sup>Laboratory of Proteomics and Analytical Technologies, SAIC-Frederick, NCI, NIH, Frederick, Maryland, USA. <sup>f</sup>Reproductive and Developmental Biology Laboratory, NIEHS, NIH, North Carolina, USA.

## Materials and Methods

**RNA Isolation and Quantitative Real-Time PCR.** Total RNA from various mouse tissues (n=10 per group) was extracted at 3 or 26 weeks of age using TRIzol reagent (Sigma-Aldrich). cDNA was reverse transcribed using oligo(dT) primers and a reverse transcription kit (Quanta Biosciences). Real-time PCR was performed using the Taqman or the Power SYBR<sup>®</sup> green PCR master mix kit (Applied Biosystems), employing an ABI QuantStudio 12K Flex Real-Time PCR System (Applied Biosystems). Real-time PCR primer sequences of *CYP19A1* and *Cyp19a1* (human and mouse aromatase), *Pgr* (mouse PR), *Colla1*, and *Gapdh* are summarized in *SI Appendix*, Table S2. The SYBR<sup>®</sup> Green-based QuantiTect mouse primers for real-time RT-PCR were from Qiagen and are listed as follows: *Esr1* (mouse ER $\alpha$ ), *Esr2* (mouse ER $\beta$ ), *Kiss1*, *Emb*, *Ren1*, *Spon2*, *Eln*, *Timp1*, *Greb1*, *Ccnd1*, *Adora1*, *Susd3*, *Tff1*, *Ar* (mouse AR), *Amd2*, *Inmt1*, and *Cyp2e1*. The Taqman-based *Gpr30* primer was purchased from IDT. Real-time PCR cycler conditions were: 50°C for 2 min, 95°C for 10 min, and 40 cycles of 95°C for 15 s and 60°C for 1

min. PCR results were normalized to the mouse *Gapdh* gene expression. Ct values at or above 40 cycles were considered to be below the level of detection.

**Exon-Specific RT-PCR Amplification.** Total RNA was extracted from abdominal muscle tissues of 26-week-old mice and cDNA was synthesized using oligo(dT) primers and a reverse transcription kit (Quanta Biosciences). To amplify the human aromatase transcript variants in the abdominal muscle driven by promoters PII/I.3 or I.4, we used forward primers designed to hybridize to the distinct 5'-untranslated region of each transcript and a reverse primer that hybridized to the common coding exon III (1). The PCR was run as follows: 4 min at 95°C, followed by 35 cycles of 30 s at 94°C, 30 s at 60°C, and 1 min at 72°C, and a final extension of 10 min at 72°C.

**Muscle Histology, Masson's Trichrome Staining, and Immunohistochemistry.** For the assessment of muscle tissue morphology and visualization of fibrosis, UAM, LAM, and QM were removed from mice and fixed in 4% phosphate-buffered paraformaldehyde, and human muscle biopsy tissues were fixed in 10% formalin overnight. Tissues were then embedded in paraffin and sectioned at 4 µm. The muscle sections were stained with H&E and examined under a microscope. The amount of fibrosis in a muscle section was determined using Masson's trichrome staining kit (American Master Tech). Using ImageJ software (NIH), 10 representative high-power fields were analyzed in each tissue. Each Masson's trichrome stained image was first converted to the RGB stack image. Next, the color channel and the image threshold were set to only show areas occupied by the connective tissue/fibrotic component or the myofiber component. The percentage of the connective tissue/fibrotic area or the myofiber area was then measured respectively. The

percentage of empty spaces were calculated and subtracted. The relative area occupied by connective tissue/fibrosis or myofibers were then calculated in proportion to the total area (2). Each area was independently calculated by two observers (H.Z. and Z.D.). Myofiber CSA in WT and Arom<sup>hum</sup> mice was quantified in more than 1,000 cells for each sample using the ImageJ software. For IHC, after deparaffinization and antigen retrieval via heating in an antigen unmasking solution (Vector Laboratories), primary antibodies (ER $\alpha$ , AR, and Ki67) were applied to the sections. After incubation at 37°C for 1 h, the sections were washed with PBS, incubated with a biotinylated secondary antibody (1:600; Vector Laboratories) at 37°C for 30 min, followed by avidin-biotin-horseradish peroxidase complex (ABC/HRP, Vector Laboratories). We then used 3,3-diaminobenzidine (DAB, Dako) as a substrate for 10 minutes, counterstained with hematoxylin, and examined the slides using a Zeiss Axio Scope microscope (Zeiss). The antibodies for IHC were purchased from the following sources: ER $\alpha$  (AJ1268a, Abgent) for mouse muscle tissue, ER $\alpha$  (RM-9101, Thermo Fisher Scientific) for human muscle tissue, PR (A0098, Dako) for both tissues, AR (RB9030, Labvision) for mouse muscle tissue, AR (M3562, Darko) for human muscle tissue, and Ki67 (ab16667, Abcam) for both tissues.

**Scoring of Immunoreactivity.** For semiquantitative analysis of immunoreactivity of steroid hormone receptors, the H-score method was used (3). Briefly, a minimum of 1,000 cells in 10 different high-power fields were counted in each tissue, and the H-score was subsequently generated by adding the percentage of strongly stained nuclei (3x), the percentage of moderately stained nuclei (2x), and the percentage of weakly stained nuclei (1x), giving a possible range of 0-300. The score was independently calculated by two of the authors (H.Z. and L.Z.) using a double-headed light microscope and researchers were blinded to the animal group allocation. In the present

study, interobserver differences were less than 5%, and the mean of the two independent values was used. Ki67 immunoreactivity was scored in more than 1,000 cells for each sample, and the percentage of Ki67 positive nuclei regardless of the immunointensity was calculated.

**Protein Extraction and Immunoblotting.** Total protein from abdominal muscle tissue of 5 WT and 5 Arom<sup>hum</sup> mice was extracted in a buffer containing 10 mmol/L Tris (pH 7.4), 150 mmol/L NaCl, 1 mmol/L EDTA, 1 mmol/L EGTA, 0.5% Nonidet P40, protease inhibitors (2 mmol/L phenylmethylsulfonyl fluoride, 10 mg/mL leupeptin, and 10 mg/mL aprotinin), and phosphatase inhibitors (100 mmol/L sodium fluoride, 10 mmol/L sodium pyrophosphate, and 2 mmol/L sodium orthovanadate). Lysates were centrifuged at 50,000 x g for 60 minutes at 4°C. Protein concentrations were determined using the BCA protein assay kit (Pierce). Samples containing 25 µg of protein were boiled for 4 minutes in reducing Laemmli sample buffer containing 80 mmol/L DTT and subjected to electrophoresis on 10% SDS-polyacrylamide gels (100 µg of protein used in Figs. 6D, S8 A and B). Proteins were then transferred from gels to nitrocellulose membranes. The membranes were blocked with 5% insulin-free BSA in TBS-Tween 20, and proteins were detected using various antibodies. After extensive washings, immune complexes were detected with horseradish peroxidase conjugated with specific secondary antiserum (Cell Signaling Technology) followed by enhanced chemiluminescence reactions. Blots were analyzed by densitometry and quantified with the ImageJ software. The antibodies were purchased from the following sources: ER $\alpha$  (04-820), EMD Millipore; type I collagen (1310-01), Southern Biotech;  $\alpha$ -SMA (A5228) and tubulin (T6793), Sigma-Aldrich; MyoD (sc-760), Santa Cruz Biotechnology; AR (ab52615), Abcam; GAPDH (AM4300), Life Technologies (Ambion); and PCNA (2586), Cell Signaling Technology.

**Serum and Tissue Hormone Levels.** Blood samples were obtained from the retro-orbital vein. Serum T, LH, and FSH levels were measured by RIA at the UVA Center for Research in Reproduction Ligand Assay and Analysis Core at the University of Virginia. Serum E<sub>2</sub> and LAM tissue estrogens (E<sub>1</sub>, E<sub>2</sub>, and E<sub>3</sub>) were determined by LC-MS<sup>2</sup> at the NCI/NIH, as described previously (1).

**Microarrays and Data Analysis.** Total RNA isolated from LAM tissues of 3-week-old WT and Arom<sup>hum</sup> mice was assessed for integrity using the Agilent Bioanalyzer 2100, and qualified RNA samples were used for the microarray experiment. Expression profiling was performed using MouseWG-6 v2.0 Expression BeadChip arrays (Illumina) following the protocol described previously (4). For each mouse genotype, four microarrays were processed. The raw expression data were normalized using the Robust Spline Normalization algorithm implemented in the lumi package in Bioconductor (5). Only the probes with a present call were considered for the analysis. Since multidimensional scaling analysis showed that a data set from samples of Arom<sup>hum</sup> mice was significantly different from those of WT mice, the differentially expressed genes were determined by the fold difference of expression level >1.5 and P-values <0.05 in WT vs. Arom<sup>hum</sup> mice. Finally, probes were mapped to genes using the nucleotide universal Identifier (nuID) annotation. The microarray data is MIAME compliant and is available at the Gene Expression Omnibus website (<http://www.ncbi.nlm.nih.gov/geo>) under accession number GSE92748.

**5'-Rapid Amplification of cDNA Ends (5'-RACE).** To determine the transcriptional start sites of human and mouse aromatase transcripts from various tissues of Arom<sup>hum</sup> mice, 5'-RACE was

performed using the SMART<sup>TM</sup> RACE cDNA amplification kit (Clontech) as described previously(1, 6). The primary touchdown PCR reverse primers used are as follows: the human aromatase touchdown reverse primer (5'-GTCCAATTCCCATGCAGTAGCCAGGA-3') and the mouse aromatase touchdown reverse primer (5'-GACTCTCATGAATTCTCCATACATCT-3'). If the primary PCR reaction failed to give distinct bands, a secondary, or “nested” PCR was performed with the human aromatase nested reverse primer (5'-CCAAGAGAAAAAGGCCAGTGAGGAGCA-3') and the mouse aromatase nested reverse primer (5'-AATGAGGGGCCCAATTCCCAGA-3'); RACE products were cloned into the pCR<sup>®</sup> - TOPO TA cloning vector and subsequently sequenced.

## References

1. Zhao H, *et al.* (2012) A humanized pattern of aromatase expression is associated with mammary hyperplasia in mice. *Endocrinology* 153(6):2701-2713.
2. Lucero HA, Patterson S, Matsuura S, & Ravid K (2016) Quantitative histological image analyses of reticulin fibers in a myelofibrotic mouse. *J Biol Methods* 3(4).
3. Ishibashi H, *et al.* (2003) Sex steroid hormone receptors in human thymoma. *The Journal of clinical endocrinology and metabolism* 88(5):2309-2317.
4. Yin P, *et al.* (2012) Genome-wide progesterone receptor binding: cell type-specific and shared mechanisms in T47D breast cancer cells and primary leiomyoma cells. *PloS one* 7(1):e29021.
5. Wang F, *et al.* (2014) Dynamic CCAAT/enhancer binding protein-associated changes of DNA methylation in the angiotensinogen gene. *Hypertension* 63(2):281-288.
6. Zhao H, *et al.* (2009) A novel promoter controls Cyp19a1 gene expression in mouse adipose tissue. *Reprod Biol Endocrinol* 7:37.

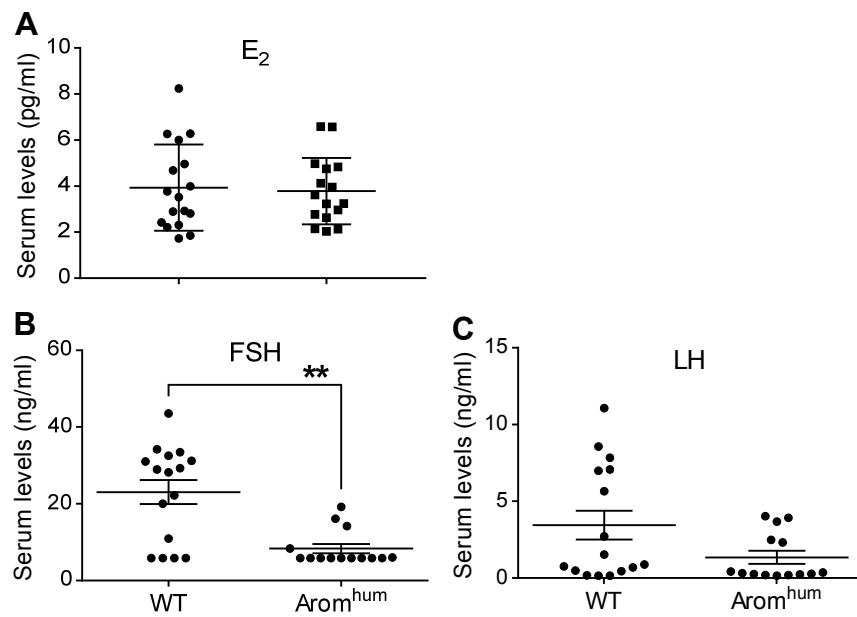


**Fig. S1. Serum levels of E<sub>2</sub>, FSH, and LH in WT and Arom<sup>hum</sup> mice.** Serum E<sub>2</sub> levels (**A**) were measured by LC-MS<sup>2</sup>. Serum levels of FSH (**B**) and LH (**C**) were measured by RIA. Mouse sera were collected from 26-week-old mice. 2-tailed Student's *t* test, \*\**P* < 0.01, n=14-17.

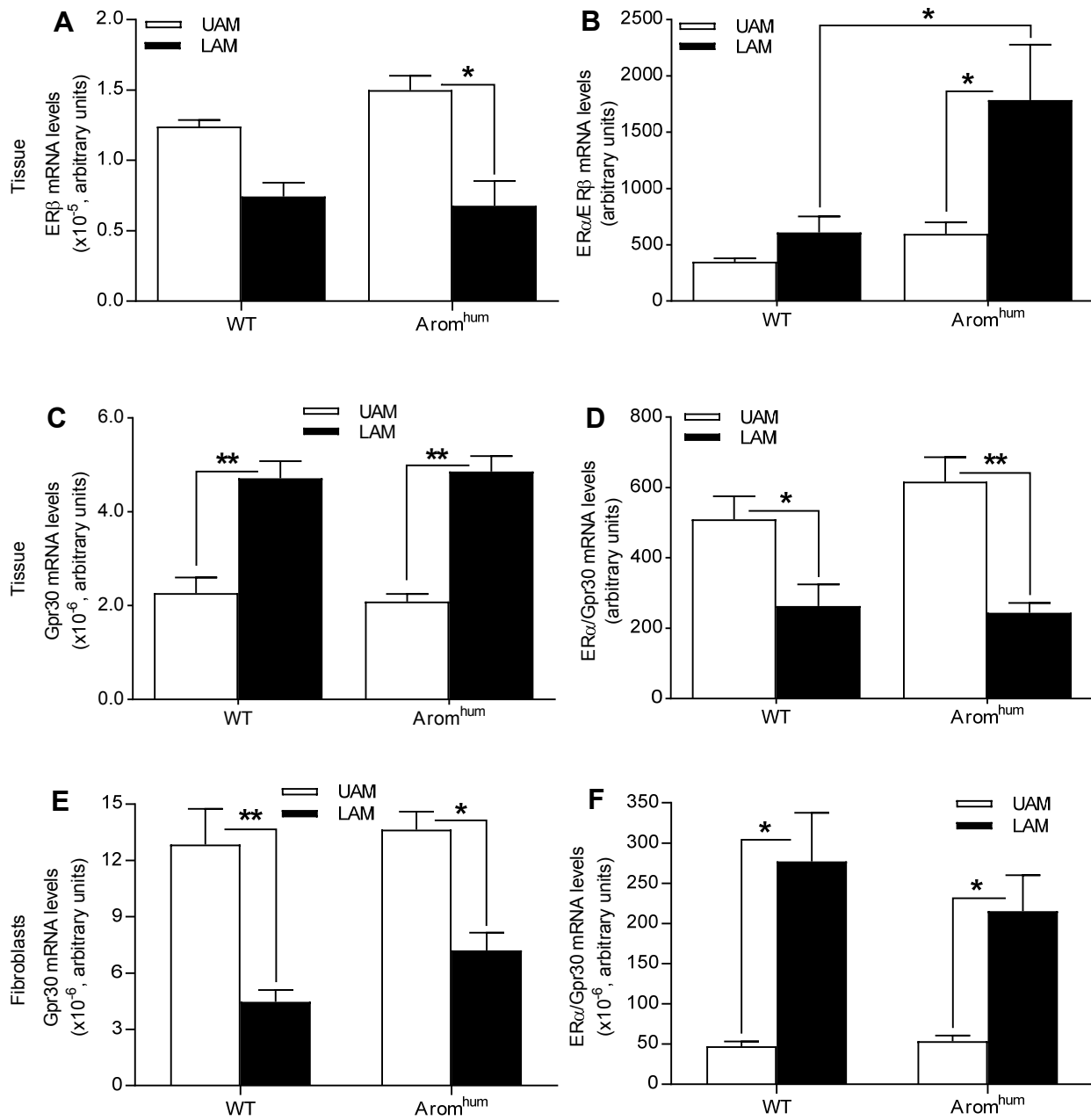


**Fig. S2.** mRNA levels of ER $\beta$  and Gpr30 in abdominal muscle tissues of 4-week-old WT and Arom<sup>hum</sup> mice. ER $\beta$  mRNA levels (**A**), the ratio of ER $\alpha$ /ER $\beta$  mRNA levels (**B**), Gpr30 mRNA levels (**C**), and the ratio of ER $\alpha$ /Gpr30 mRNA levels (**D**) in UAM and LAM tissues.  $n=8$  mice per group. Gpr30 mRNA levels (**E**) and the ratio of ER $\alpha$ /Gpr30 mRNA levels (**F**) in primary fibroblasts from UAM and LAM tissues of WT and Arom<sup>hum</sup> mice.  $n=6$  mice per group. Two-way ANOVA with Tukey's multiple comparison test,  $*P < 0.05$ ,  $**P < 0.01$ .



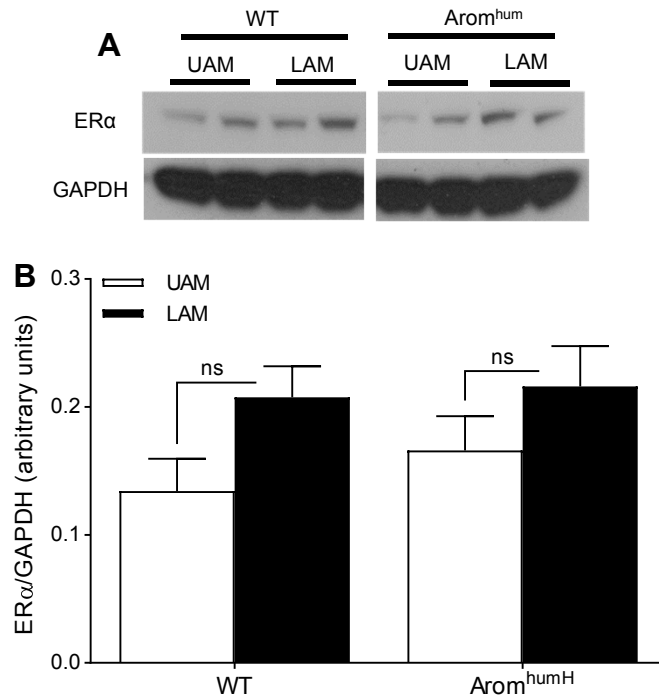


**Fig. S3.** (A) ER $\alpha$  protein levels were detected by immunoblotting in UAM and LAM tissues of WT and Arom<sup>hum</sup> mice. GAPDH protein levels served as the control. All samples were run on the same gel but were noncontiguous. (B) ER $\alpha$  protein levels were quantified by densitometry. Two-way ANOVA with Sidak's multiple comparison test,  $P = 0.2651$  for UAM vs. LAM in WT mice and  $P = 0.4264$  for UAM vs. LAM in Arom<sup>hum</sup> mice,  $n=5$ ; ns, not significant.

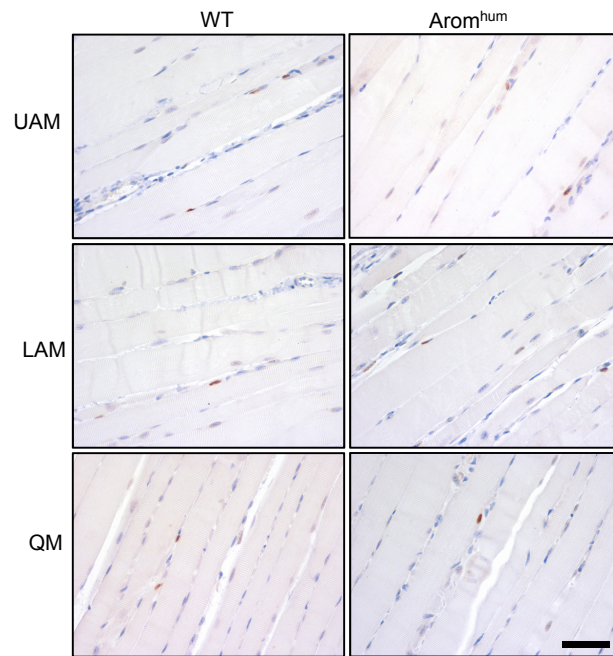


**Fig. S4. ER $\alpha$  expression in myocytes of UAM, LAM (area unaffected by hernia), and QM of WT and Arom<sup>hum</sup> mice was measured by IHC staining.**  
Scale bar, 50  $\mu$ m. n =10 in each group.

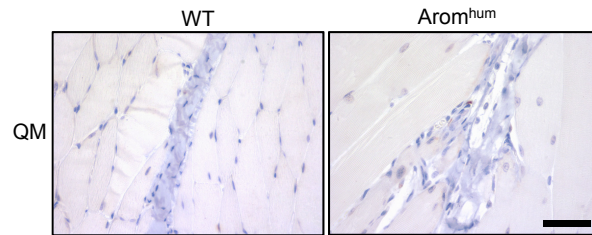


**Fig. S5. ER $\alpha$  expression in QM stroma of WT and Arom<sup>hum</sup> mice was measured by IHC staining. Scale bar, 50  $\mu$ m. n =8-10 in each group.**

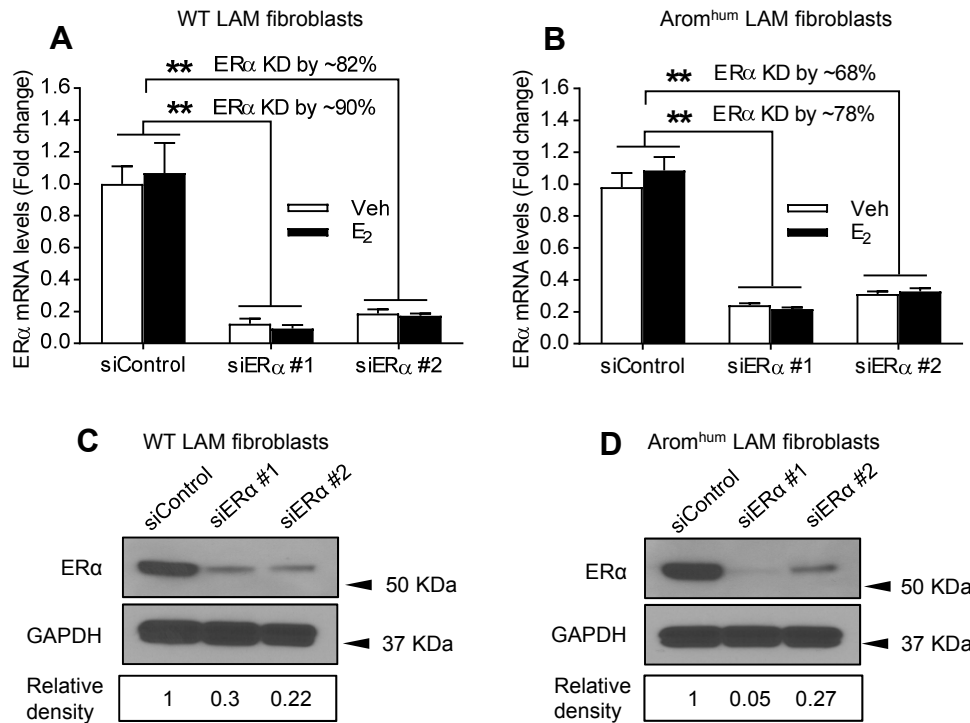


**Fig. S6. ER $\alpha$  mRNA and protein levels after siRNA-mediated knockdown in primary LAM fibroblasts of WT and Arom<sup>hum</sup> mice.** ER $\alpha$  mRNA levels in primary fibroblasts from WT LAM tissue (A) and Arom<sup>hum</sup> LAM tissue (B). ER $\alpha$ -knockdown fibroblasts were treated with vehicle (Veh) or E<sub>2</sub> (10 nM) for 24 hours before harvesting cells for extracting RNA. GAPDH mRNA levels served as the control. KD, knockdown. Two-way ANOVA with Tukey's multiple comparison test, \*\*P < 0.01, n=6 mice in each group. ER $\alpha$  protein levels in primary fibroblasts from WT LAM tissue (C) and Arom<sup>hum</sup> LAM tissue (D) after siRNA-mediated ER $\alpha$  knockdown. The data shown in C and D are representative of 3 independent experiments.

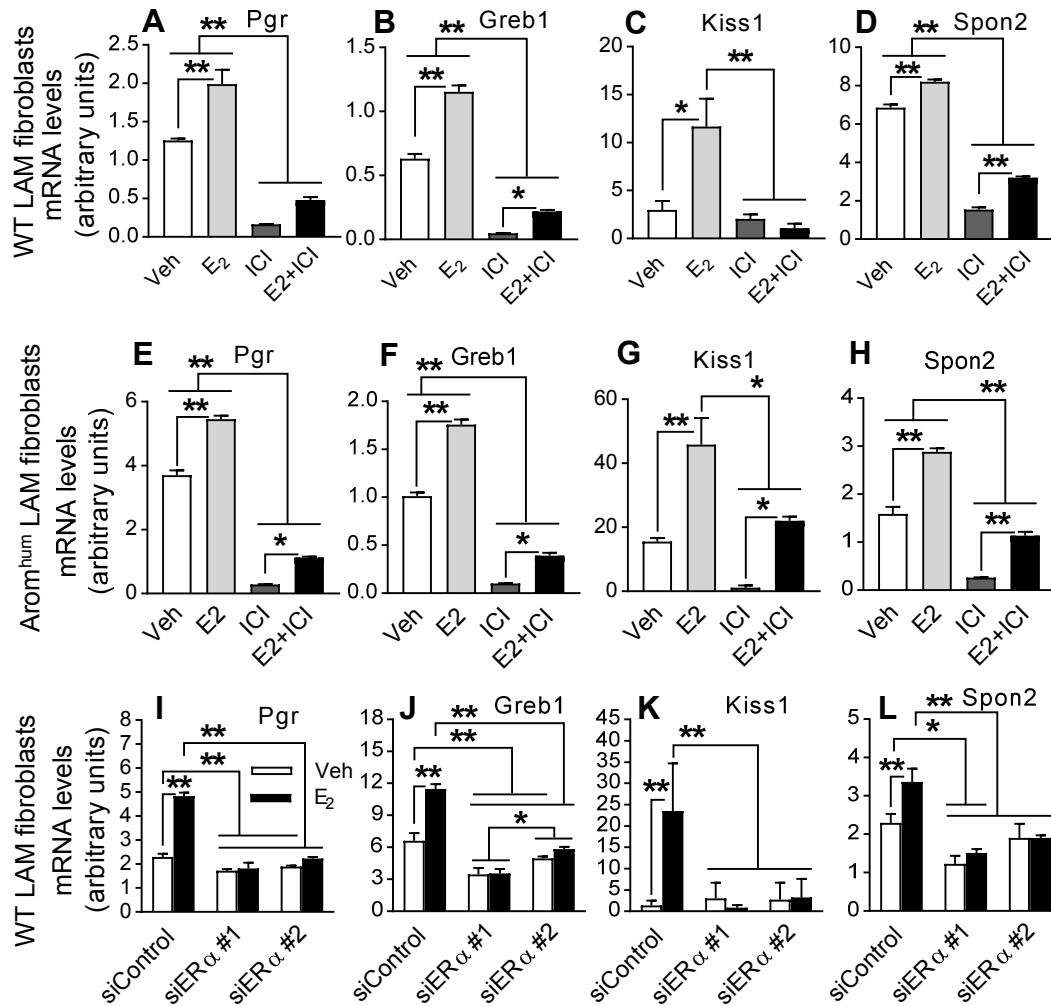


**Fig. S7. Increased ER $\alpha$  expression in LAM tissue are responsible for increased expression of estrogen-responsive and fibrotic genes in WT and Arom<sup>hum</sup> mice.** mRNA levels of *Pgr*, *Greb1*, *Kiss1*, and *Spon2* in primary LAM fibroblasts from WT (A, B, C, and D) and Arom<sup>hum</sup> (E, F, G, and H) mice after 100-nM ICI 182780 (ICI) treatment in the presence or absence of E<sub>2</sub> (10 nM). Cells were pretreated with ICI 182780 for two hours before the addition of E<sub>2</sub>. mRNA levels of *Pgr*, *Greb1*, *Kiss1*, and *Spon2* in primary LAM fibroblasts from WT mice after siRNA-mediated knockdown of ER $\alpha$  (I, J, K, and L) in the presence or absence of E<sub>2</sub> (10 nM). Veh: vehicle. GAPDH mRNA levels served as controls. One-way ANOVA with Sidak's multiple comparison test for A-H. Two-way ANOVA with Tukey's multiple comparison test for I-L. \*P < 0.05, \*\*P < 0.01, n=6 mice in each group.

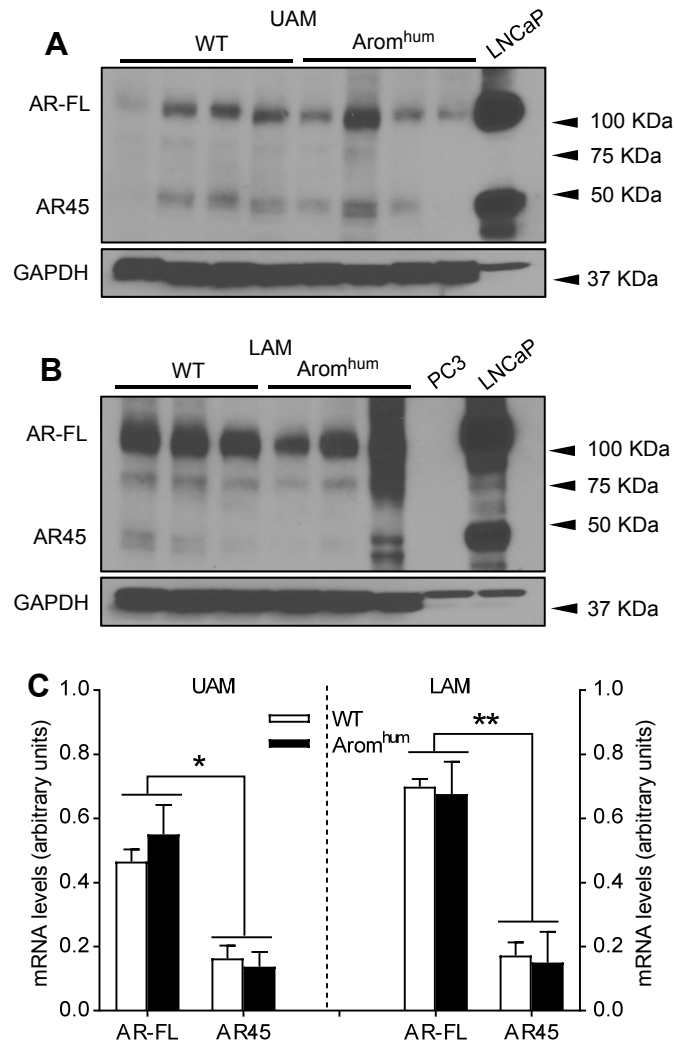


**Fig. S8.** Protein levels of AR-FL and AR45 between WT and Arom<sup>hum</sup> mice were defined by immunoblotting in UAM (**A**) and LAM (**B**) tissues. GAPDH protein levels served as the loading control. Prostate cancer cell lines LNCaP and PC3 served as positive and negative controls for AR-FL and AR45. (**C**) Quantification of AR-FL and AR45 by densitometry in UAM and LAM of WT and Arom<sup>hum</sup> mice. Two-way ANOVA with Sidak's multiple comparison test, \* $P < 0.05$ , \*\* $P < 0.01$ .  $n=3-4$  mice in each group.

**Table S1. mRNA expression profile of human aromatase in various tissues of 26-week-old male Arom<sup>hum</sup> mice.**

Tissues (n=3)	WT		Arom <sup>hum</sup>	
	H Arom	M Arom	H Arom	M Arom
Testis	–	Pgon	PII	Pgon
Epididymis	–	Pgon/Ptes	PII	Pgon/Ptes
Hypothalamus	–	Pbr	I.f	Pbr
Gonadal fat	–	Padi	PII	Padi
Pituitary	–	–	+	–
Aorta	–	–	I.4	–
Lung	–	–	I.4	–
Bladder	–	–	I.4	–
Abdominal muscle	–	–	I.4 (PII*)	–
Quadriceps muscle	–	–	I.4(PII*)	–
Stomach	–	–	+	–
Subcutaneous fat	–	–	+	–
Brown adipose	–	–	+	–
Heart	–	–	+	–
Liver	–	–	+	–
Spleen	–	–	+	–
Intestine	–	–	I.7/I.f	–
Kidney	–	–	+	–
Bone	–	–	I.4	–

Quantitative real-time RT-PCR was used to determine the presence (+) or absence (-) of mouse and human aromatase mRNA in various tissues of WT and Arom<sup>hum</sup> mice. 5'-RACE identified mRNA transcribed from each promoter (PII, I.f, I.4, I.3) in the human aromatase transgene or native mouse promoters. The term “present (+)” only denotes the amplification of the coding region of human aromatase mRNA species by real-time PCR; we were, however, unable to detect the promoter-specific 5'-untranslated regions in these tissues using 5'-RACE. If 5'-RACE produced a promoter-specific mRNA, this promoter was indicated in the table. \*The promoter PII usage in abdominal and quadriceps muscle tissue was low and detectable only by exon-specific RT-PCR. Pgon=mouse gonadal aromatase promoter; Ptes=mouse testis aromatase promoter; Pbr=mouse brain aromatase promoter; Pad=mouse gonadal fat aromatase promoter; H Arom=human aromatase; M Arom=mouse aromatase.

**Table S2. Real-time PCR primers used in the study.**

<b>Gene symbol</b>	<b>Forward primer</b>	<b>Reverse primer</b>
CYP19A1	CACATCCTCAATACCAGGTCC Probe (6FAM-CCCTCATCTCCCACGGCAGATTCC-TAMRA QUENCHER 3' SP LINKED)	CAGAGATCCAGACTCGCATG
Cyp19a1	GCCCTTTCTTTATGAAAGCTC	AGGCGTTAAAGTAACCCTGGA
Pgr	GACTGGCTGTGGAATTTCC	CCAGGATCTGGGCAACTG
Col1a1	GCAAGAATGGCGATCGTG	ATGCCTCTGTACCTTGTTCC
Gapdh	ATCTTCTTGTGCAGTGCCAGC	GTTGATGGCAACAATCTCCAC